

# Physical Interpretation of the Influence of a DC Discharge on a Supersonic Rarefied Flow over a Flat Plate

V. Lago<sup>a</sup>, J.C. Lengrand<sup>a</sup>, E. Menier<sup>a</sup>, T.G. Elizarova<sup>b</sup> and A.A. Khokhlov<sup>c</sup>

<sup>a</sup>*CNRS/ICARE, 1C avenue de la recherche scientifique, 45071 Orléans Cedex 2, France*

<sup>b</sup>*Institute for Mathematical Modeling, Russian Academy of Sciences, Miusskaya sq.4a, 125047 Moscow, Russia*

<sup>c</sup>*Dept of physics, Moscow State University, Vorobiev Gory, 119899 Moscow, Russia*

**Abstract.** The present work is an attempt to clarify the physical interpretation of the changes in flow parameters and dynamic loads induced by an electric discharge in the vicinity of a flying body. The particular case considered here is a sharp flat plate in a low-density flow at Mach 2. The problem has been studied both experimentally and numerically. It is concluded that the change in wall temperature due to the discharge explains best the changes observed in the distribution of Pitot pressure. The observed changes in dynamic loads due to the discharge cannot be explained by the distribution of wall normal and tangential stresses. Coulomb forces between the gas and the electrodes mounted on the wall are probably also involved.

**Keywords:** Electric discharge, ionic wind, DSMC, flow control, rarefied gas dynamics.

**PACS:** 47.40.Ki; 47.45.-n; 47.85.L-

## INTRODUCTION

The influence of an electric discharge on the aerodynamic properties of a flow has been studied for many years. A review of these works for subsonic applications is given, e.g., by Moreau [1] and the role of ionic wind on slender bodies (wing profiles) is often pointed out. For supersonic flows, reviews have been given, e.g., by Bletzinger et al. [2] and by Fomin et al. [3]. Most attention has been paid to weakening the shock wave in front of blunt bodies and the phenomena observed are often interpreted by purely thermal effects. The present work aims at clarifying the physical interpretation of the changes in flow parameters and dynamic loads induced by an electric discharge in the vicinity of a flat plate under rarefied supersonic conditions. It has been initiated a few years ago at the *Laboratoire d'Aérothermique du CNRS* (now included in the *Institute for Combustion, Aérothermique, Réactivité et Environnement*), in cooperation with the *Institute for Mathematical Modeling of the Russian Academy of Sciences*.

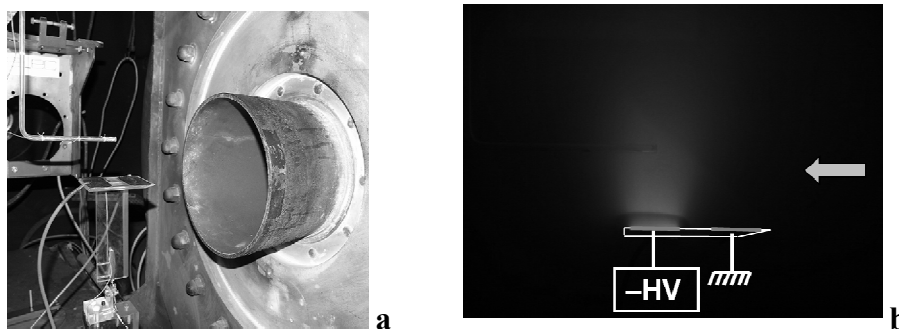


FIGURE 1. a - Nozzle and model, b – Visualization of the discharge.

Experiments have been carried out in the MARHy facility of ICARE (Fig.1a): The working gas was air, flowing at a nominal Mach number of 2. The stagnation temperature was room temperature and the stagnation pressure was equal to 63 Pa. The obstacle was a sharp flat plate, 100 mm long and 80 mm wide. It was made of quartz, with two

thin electrodes glued on its surface, 20 mm apart from each other. One electrode was grounded and the other one (active electrode) was connected to a high-voltage source. When the active electrode was positive it was impossible to obtain a stable discharge: arcs and sparks appeared on all metallic parts of the wind-tunnel. When the active electrode was negative a stable glow discharge was obtained above the plate (Fig.1b), with a violet emission due to de-excitation of excited nitrogen states. Either the downstream or upstream electrode could be active.

Experimental measurements included Pitot pressure distribution in the flowfield and infrared thermography of the plate. In addition, a strain gauge mounted on the model sting gave access to the pitching moment.

In parallel, a numerical work was carried out for the same flow conditions using a molecular approach (Direct Simulation Monte Carlo: DSMC). The DSMC approach was presented in [4]. Preliminary results and details on the experiment have been presented in [4], [5], [6].

The present paper comes after additional experimental work:

- An electrostatic probe was used to get the distribution of electric potential in the flowfield.
- A high-speed camera was used for time-resolved flowfield visualization (Fig. 1b).

The numerical work was completed by a continuum approach (Navier-Stokes equations) under the usual (NS) or the Quasi GasDynamic (QGD) formulation [7]. In the present case the additional terms in QGD compared with NS act as artificial viscosity. Velocity slip and temperature jump were accounted for.

To investigate the influence of the downstream boundary condition, some DSMC, NS and QGD calculations were done for a plate somewhat longer than the actual one.

The reference flowfield without a discharge was treated, resulting in nearly identical NS, QGD and DSMC results (Fig.2a), as expected for the rarefaction level under investigation. The agreement with experiment had been confirmed earlier [4] by comparing measured and calculated Pitot pressure distributions.

There has been no attempt to model the discharge itself. However a number of numerical computations were carried out to simulate different possible effects of the discharge, namely ionic wind, energy input, change in wall temperature.

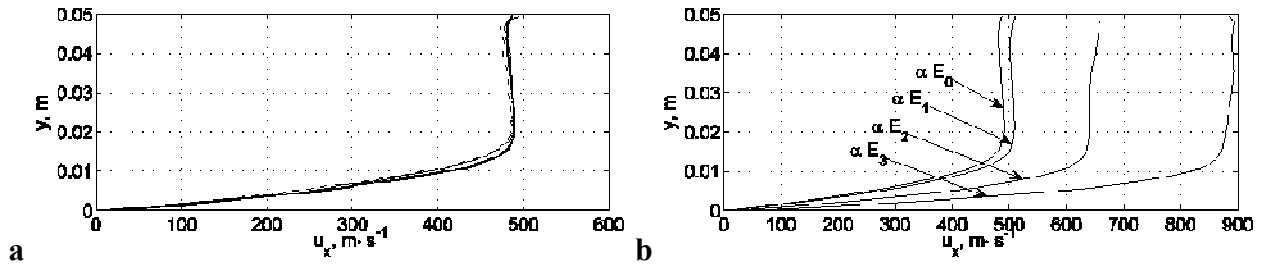


FIGURE 2. Longitudinal velocity profile at  $x = 100$  mm from leading edge, obtained

a) by DSMC (thin full line), QGD (thick full line) and NS (dashed line)

b) by QGD with a volume force due to electric field:  $\alpha E = 0$  ( $\alpha E_0$ ),  $0.03 \text{ V} \cdot \text{m}^{-1}$  ( $\alpha E_1$ ),  $0.3 \text{ V} \cdot \text{m}^{-1}$  ( $\alpha E_2$ ), and  $1 \text{ V} \cdot \text{m}^{-1}$  ( $\alpha E_3$ ).

## MODELING IONIC WIND

When the DC discharge is switched on, ions are accelerated according to the local electric field and transfer momentum to neutral species through collisions, thus modifying the mean flow velocity. This is ionic wind.

A number of DSMC calculations were carried out and included the process of ion acceleration and momentum transfer. The gas was considered as a mixture of neutral molecules  $N_2$  and molecular ions  $N_2^+$ , whose respective concentrations were imposed when injecting particles through boundaries. The objective was to decide whether this process was sufficient to create a change in the velocity distribution and in the aerodynamic properties of the model. Preliminary calculations [4] were based on a uniform electric field (parallel to the plate) all over the computational domain. They allowed to conclude that the electric field was insufficient to modify the flowfield or the aerodynamic properties, unless the ionization fraction was chosen unrealistically high.

QGD calculations were also carried out to simulate the role of the electric field, by introducing a volume force ( $n e \alpha E$ ) per unit-volume, where  $n$  is the number density,  $e$  the electron charge,  $\alpha$  the ionized fraction and  $E$  the electric field. The momentum and the energy equations were modified accordingly. A parametric study was carried out by varying the product ( $\alpha E$ ) and lead to the same conclusion (Fig.2b). A departure from the reference case begins to appear at  $\alpha E = 0.03 \text{ Vm}^{-1}$ , whereas realistic values would be lower.

DSMC computations have been repeated with a tentatively more realistic electric field distribution, obtained by solving the Laplace equation, based on the location of the electrodes. The calculation of the electric field covered a

domain much larger than the DSMC domain. Neumann conditions were imposed on all boundaries except the electrodes. The electric field was characterized by  $\Delta V/L$ , where  $\Delta V$  is the potential difference and  $L$  the distance between electrodes. It was expected that the governing parameter for modeling ionic wind was the product ( $\alpha \Delta V/L$ ). The parameter ( $\Delta V/L$ ) was taken equal to  $15 \text{ V.m}^{-1}$ , much lower than the actual one ( $50 \text{ kV.m}^{-1}$ ) to keep the velocity change small during a DSMC time step. The ionized fraction  $\alpha$  was taken equal to  $10^{-2}$  and  $10^{-1}$ , much larger than its actual value. An influence of the electric field was observed on DSMC results for  $\alpha \Delta V/L = 0.15 \text{ V.m}^{-1}$  and higher. For a realistic value  $\Delta V/L = 50 \text{ kV.m}^{-1}$ , this would correspond to an ionized fraction  $\alpha = 3 \cdot 10^{-6}$ , which is probably larger than the actual one.

Furthermore, an experimental survey of the flowfield by an electrostatic probe reveals that the potential distribution does not correspond to the solution of the Laplace equation. It is nearly uniform and close to  $-25 \text{ V}$ , except in the immediate vicinity of the active electrode (Fig.3). Thus the above calculations tend to overestimate the electric field.

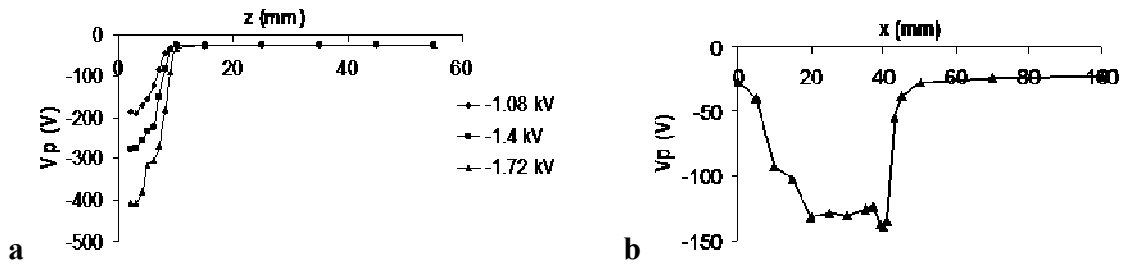


**FIGURE 3.** Electric potential measured by an electrostatic probe  
a – transverse profile above the cathode, b – longitudinal profile above the cathode, 5 mm from the plate surface for  $V = 1.08 \text{ kV}$ .

Finally, preliminary DSMC calculations [4] indicated that the effect of the electric field does not really depend on the product ( $\alpha \Delta V/L$ ). It depends more on  $\alpha$  than on  $\Delta V/L$ . By computing the flowfield with an artificially low  $\Delta V/L$  and an artificially large  $\alpha$ , we overestimate even more the influence of the electric field. We can thus conclude that ionic wind plays a negligible role under the considered conditions.

## MODELING ENERGY INPUT

The discharge contributes to an input of energy to the flow. In the experiment, the power passed to the gas, based on the voltage and current applied to the electrodes is in the range 0-90 W. DSMC calculations with energy input were carried out for pure nitrogen and presented in [4]. The range of energy input per unit-volume in the computation ( $0\text{-}80 \text{ kW.m}^{-3}$ ) corresponds approximately to the experimental one. There was virtually no influence on the flowfield for energy input less than  $5 \text{ kW.m}^{-3}$ . However, a clear influence was observed for  $80 \text{ kW.m}^{-3}$ .

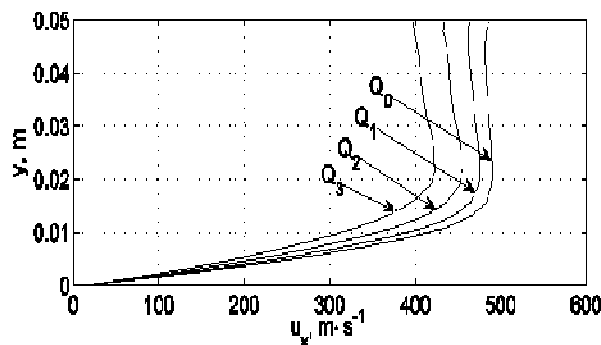


**FIGURE 4.** QGD velocity profiles at  $x = 100 \text{ mm}$  from leading edge obtained with energy input equal to  $0 \text{ kW.m}^{-3}$  ( $Q_0$ ),  $20 \text{ kW.m}^{-3}$  ( $Q_1$ ),  $50 \text{ kW.m}^{-3}$  ( $Q_2$ ),  $100 \text{ kW.m}^{-3}$  ( $Q_3$ ).

Similar computations were repeated with the QGD approach. The energy equation was modified by an additional term to account for energy input. The results presented in Fig.4 are consistent with the previous conclusion based on DSMC calculations.

However even if the total energy input in the simulations is representative of the experimental one, both DSMC and QGD calculations fail to reproduce the correct spatial distribution of the energy input. The latter takes place essentially near the cathode, rather than being distributed uniformly. Furthermore, a part of the discharge energy is trapped as vibrational energy in the gas and relaxes far downstream, without influencing the flowfield around the plate. Thus both DSMC and QGD calculations overestimate the influence of energy input.

## WALL TEMPERATURE

In all above-mentioned calculations, the wall temperature was kept equal to room temperature. However the discharge tends to heat the wall, which affects the boundary layer thickness and all the flowfield. During experiments, the plate was observed by an infrared camera and the wall temperature distribution was recorded, assuming an emissivity coefficient of unity for the quartz surface. The emissivity coefficient for the aluminum electrodes is close to zero and it was not possible to measure directly the electrode temperature. Therefore a small spot on the electrodes was covered with a black paint and the temperature of this spot could be measured. It was supposed to be representative of that of the underlying electrode. A detailed discussion of wall heating is presented in [6]. It is attributed to ionic bombardment of the cathode, which heats the cathode. Then the rest of the plate is heated by wall conduction from the cathode. A steady state is obtained with maximal temperatures observed on the active electrode as indicated in Table 1. The electrode temperature is higher when the upstream electrode is active.

TABLE 1. Maximal temperature observed on the active electrode.

Electric power injected	Upstream electrode active	Downstream electrode active
30 W	473 (+/-3) K	442 (+/-2) K
60/59 W	537 (+/-4) K	526 (+/-4) K
94/90 W	656 (+/-5) K	633 (+/-4) K

DSMC computations were carried out to estimate how the change in wall temperature influences the flowfield. The standard version of the code was used, without modification for electric field or energy input. The wall temperature  $T_w$  was prescribed to a value suggested by the above-mentioned experiments. The simulation was somewhat simplified: the wall temperature was assumed to be uniform, whereas in the experiments there is a maximum on the active electrode. An example of the results obtained by DSMC is presented in Fig.5. A higher wall temperature corresponds to a thicker boundary layer, in accordance with boundary layer theory. The change is already noticeable for the wall temperature that corresponds to a 60W discharge.

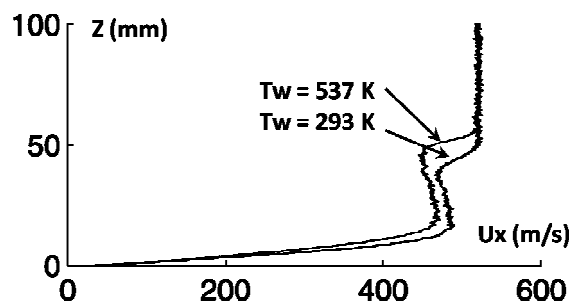
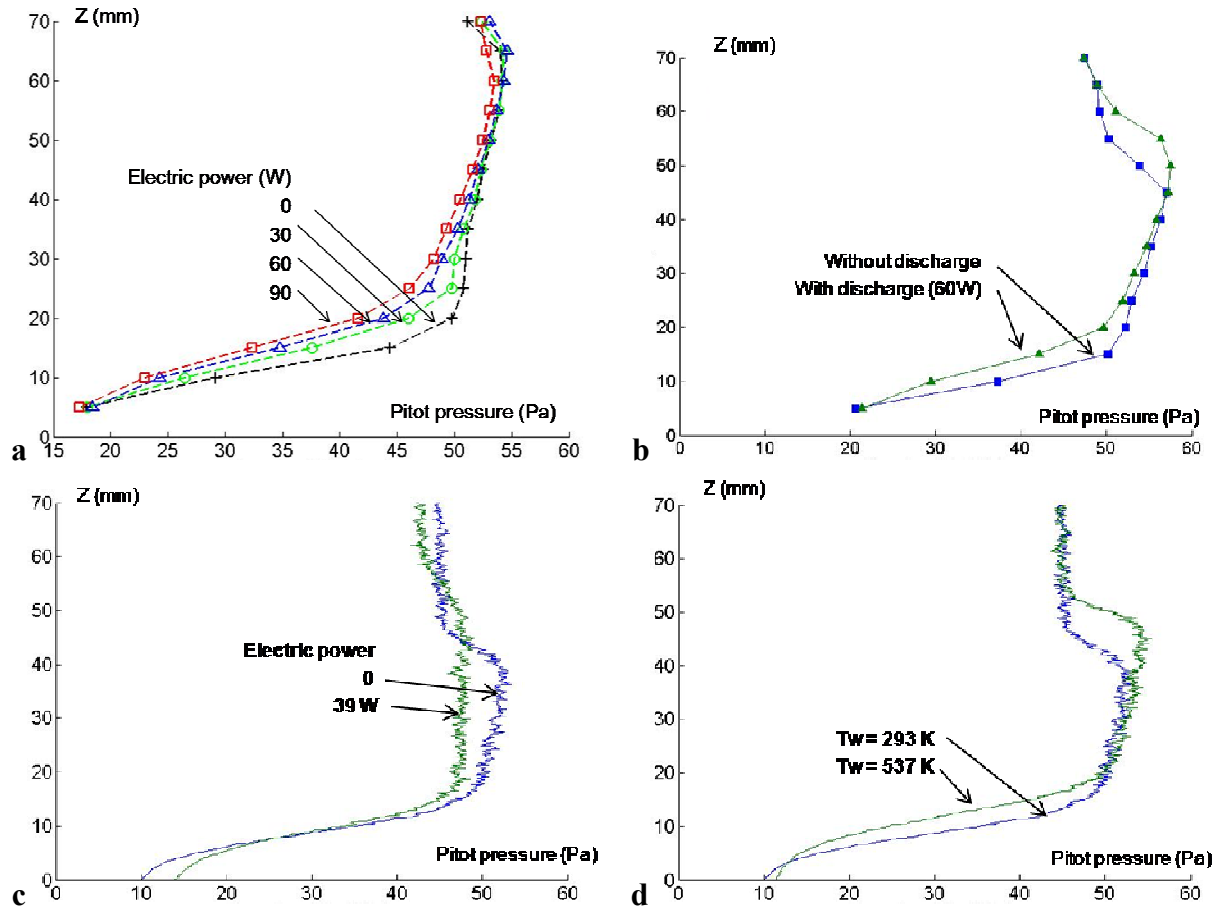


FIGURE 5. Profile of axial velocity at  $x = 49.5$  mm from leading edge (i.e. between the electrodes).

## INTERPRETATION OF PITOT PRESSURE MEASUREMENTS

Pitot pressure surveys were carried out for three values of the electric power input (30, 60 and 90 W) and two variants of the active electrode (cathode upstream or downstream) [6]. An example of results is presented in Fig. 6a. The thickness of the boundary layer increases as the electric power of the discharge increases. This effect is clearly visible when the upstream electrode is active and less visible when the downstream electrode is active.

For interpretation purpose, the change in Pitot pressure distribution is also presented in Fig.6 as it results b) from experiment, c) from DSMC with energy input, d) from DSMC with heated wall. The profiles for b), c), d) were taken near the middle of the plate ( $x = 49.5$  mm). It is clear from Fig. 6bcd that the change in Pitot pressure profile is reproduced better by wall heating than by volume energy input.



**FIGURE 6.** Transverse distribution of Pitot pressure a) above the downstream electrode (experiment, upstream electrode active) b) experiment (upstream electrode active) c) DSMC (energy input), d) DSMC (wall heating).

## DYNAMIC LOADS

The experience does not allow a detailed measurement of model lift and drag. However, the strain gauge installed on the sting gives access to the pitching moment  $M$  exerted by the flow to the model. The moment is taken with respect to the gauge location and counted positively when it tends to increase the angle of attack.

The calculation gives access to the wall distribution of normal and tangential stress. Then the pitching moment can be calculated. A direct comparison with experiment is not possible, because the calculation considers only the flow above the plate, while the experiment measures the dynamic loads on both faces and on the sting. However, the difference in dynamic loads when discharge is on or off is comparable. The comparison can be only qualitative due to a small error in the gauge calibration procedure.

The changes in the distributions of normal and tangential stresses when the wall temperature changes from 293 (reference) to 537 K are shown in Fig.7, resulting from the DSMC calculations. The last two centimeters of the plate are affected by inadequate downstream boundary condition and should be disregarded.

The changes  $\Delta M$  in the pitching moment are presented in Table 2, as obtained a) from the experiment, b) from DSMC with and without energy input, c) from DSMC for different values of wall temperature. Calculated values are presented for a plate width of 8 cm, as in the experiment. The calculation allowed estimating separately the changes of pitching moment  $\Delta M_n$  and  $\Delta M_t$  due to normal and tangential stresses, respectively.

In the calculated results, the pitching moment changes are due essentially to changes in pressure distribution (normal stress) rather than to changes in shear stress. All simulations result in a negative variation while experiments reveal a positive variation. This difference may be explained as follows. The model is submitted not only to aerodynamic forces but also to Coulomb forces between the flow and the electrodes. The Coulomb forces have not

been considered here and would be zero only in the case of electro-neutrality of the gas, which is not guaranteed in the present case.

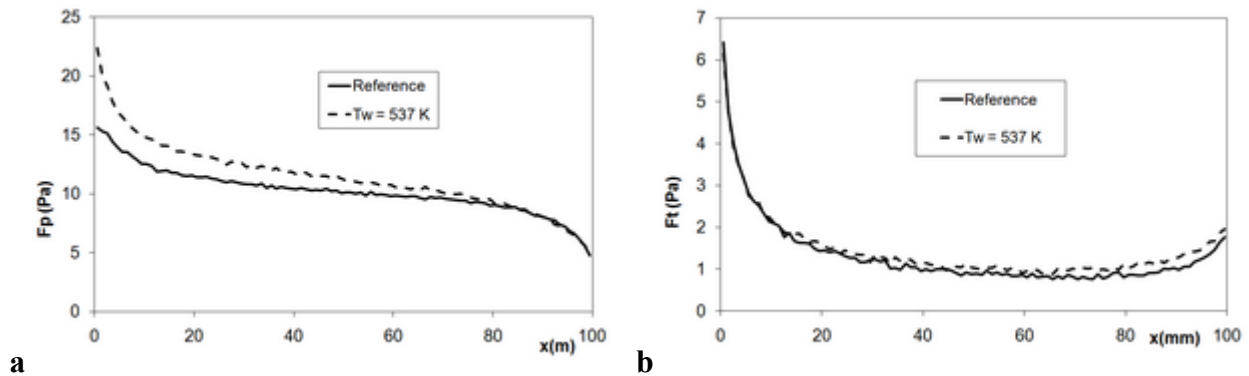


**FIGURE 7.** Distribution of (a) normal and (b) tangential stresses along the plate. DSMC calculation for 2 values of  $T_w$ .

**TABLE 2.** Changes in pitching moment: experiment and simulations.

	$\Delta M_n$ (N.m)	$\Delta M_t$ (N.m)	$\Delta M$ (N.m)
<b>Experiment</b>			
cathode upstream 30W			$\approx 0$
cathode upstream 60W			$4.7 \cdot 10^{-4}$
cathode upstream 90W			$7.6 \cdot 10^{-4}$
cathode downstream 30W			$\approx 0$
cathode downstream 60W			$1.0 \cdot 10^{-4}$
cathode downstream 90W			$1.2 \cdot 10^{-4}$
<b>DSMC</b>			
energy input 39 W	$-7.67 \cdot 10^{-5}$	$-3.15 \cdot 10^{-5}$	$-1.08 \cdot 10^{-4}$
energy input 78 W	$-3.79 \cdot 10^{-4}$	$-6.67 \cdot 10^{-5}$	$-4.46 \cdot 10^{-4}$
wall temperature 414 K	$-1.51 \cdot 10^{-4}$	$8.84 \cdot 10^{-5}$	$-6.30 \cdot 10^{-5}$
wall temperature 537 K	$-2.97 \cdot 10^{-4}$	$1.78 \cdot 10^{-4}$	$-1.19 \cdot 10^{-4}$

## CONCLUSION

Experiments have confirmed that an electric discharge induces changes in a supersonic rarefied flowfield along a flat plate model. It results from numerical simulations that these changes are due essentially to the change in wall temperature when the discharge is switched on. However the change in pitching moment cannot be explained by aerodynamic loads only. The role of Coulomb forces due to a violation of electro-neutrality is suggested.

## REFERENCES

1. E. Morean, *J. of Physics D: Applied Physics* **40**, 605-636 (2007).
2. P. Bletzinger, B.N. Ganguly, D.Van Wie, A. Garscaden, *J. of Physics D: Applied Physics* **39**, 33-57 (2005).
3. V.M. Fomin, P.K. Tretyakov, J.P. Taran, *Aerospace Science and Technology* **8**, 411-421 (2004).
4. E. Menier, J.C. Lengrand and V. Lago, "DSMC Estimate of the Ionic Wind Effect on a Supersonic Low-Density Flow " in *Proc. of the 25th Intern. Symp. on Rarefied Gas Dynamics*, edited. by M.S. Ivanov & A.K. Rebrov, Publishing House of the SBRAS, Novosibirsk, 2007, pp.402-407.
5. E. Menier, E. Depussay, L. Leger, V. Lago and J.C. Lengrand, " Modification of a Rarefied Supersonic Flow over a Flat Plate Using an Electrical Discharge ", in *Proc. of the 25th Intern. Symp. on Rarefied Gas Dynamics*, edited. by M.S. Ivanov & A.K. Rebrov, Publishing House of the SBRAS, Novosibirsk, 2007, pp.604-609.
6. E. Menier, V. Lago, E. Depussay, J.C. Lengrand, " Influence of a DC discharge on a supersonic rarefied air flow over a flat plate: experimental study", Proc. on CD-ROM, 2<sup>nd</sup> European Conf. for Aerospace Sciences (EUCASS), Brussels (Be), June 1-6, 2007.
7. A. Chpoun, T.G. Elizarova, I.A. Graur, J.C. Lengrand, *European Journal of Mechanics B/Fluids* **24** 457-467 (2005).